

A FIB/TEM STUDY OF PARTICLE C0076-FO004 RETURNED FROM THE ASTEROID RYUGU, WITH A FOCUS ON THE STRUCTURES AND COMPOSITIONS OF SULFIDE GRAINS. J. Han¹, M. Zolensky², J. Martinez³, A. J. Brearley⁴, T. Nakamura⁵, T. Morita⁵, M. Kikuri⁵, K. Amano⁵, E. Kagawa⁵, H. Yurimoto⁶, T. Noguchi⁷, R. Okazaki⁸, H. Yabuta⁹, H. Naraoka⁸, K. Sakamoto¹⁰, S. Tachibana^{10,11}, S. Watanabe¹², and Y. Tsuda¹⁰.

¹Department of Earth and Atmospheric Sciences, University of Houston, Houston, TX 77204, USA (jhan28@central.uh.edu), ²ARES, NASA Johnson Space Center, Houston, TX 77058, USA, ³Jacobs, NASA Johnson Space Center, Houston, TX 77058, USA, ⁴University of New Mexico, Albuquerque, NM 87131, USA, ⁵Tohoku University, Sendai 980-8578, Japan, ⁶Hokkaido University, Sapporo 060-0810, Japan, ⁷Kyoto University, Kyoto 606-8502, Japan, ⁸Kyushu University, Fukuoka 812-8581, Japan, ⁹Hiroshima University, Higashi-Hiroshima 739-8526, Japan, ¹⁰ISAS/JAXA, Sagami-hara 252-5210, Japan, ¹¹The University of Tokyo, Tokyo 113-0033, Japan, ¹²Nagoya University, Nagoya 464-8601, Japan.

Introduction: Samples from the C-type asteroid Ryugu were returned to Earth by the Hayabusa 2 mission. There were two touch-down samplings [1]: Chamber A sample represents the uppermost surface materials of Ryugu and Chamber C sample represents the subsurface and ejecta materials collected near an artificial crater so expected to have never experienced a long-term exposure to space. Initial laboratory analyses of these materials demonstrate that they are primordial particles dominated by volatile- and organic-rich materials, similar to CI chondrites [e.g., 2-4]. Thus, detailed analyses of the Ryugu samples will provide unique insights into the origin and early evolution of our Solar System and the building blocks of life.

Here we present preliminary FIB/TEM results of a mineralogical, chemical, and microstructural study of one Ryugu particle and compare these observations with those of CI chondrites. Sulfides are sensitive indicators of low-temperature aqueous alteration so that we focused on their structure and compositions to provide constraints on aqueous alteration conditions that the parent asteroid of Ryugu experienced.

Methods: The Ryugu particle C0076-FO004 from Chamber C was hand-picked using epoxy and attached to the top of the epoxy bullet. With the sample surface partially exposed by the microtomy technique, initial mineralogical survey of the particle was performed using a Supra 55 variable pressure field emission SEM and Bruker EBSD system. Two FIB sections from the particle were prepared using a FEI Quanta 3D field emission SEM/FIB; the first section was prepared normal to the elongation direction of a pyrrhotite lath and the second section was prepared from magnetite and adjacent carbonate. The sections were examined using a JEOL 2500SE field emission STEM equipped with a JEOL silicon drift detector for EDX analyses.

Selected area electron diffraction (SAED) patterns, as well as Fast Fourier transform (FFT) patterns extracted from high-resolution TEM images, obtained from individual sulfide grains were carefully indexed based on the space group setting and lattice parameters for the 4C, 5C, and 6C pyrrhotite superstructures,

pentlandite, and troilite for their phase identification. The actual SAED patterns were verified with those simulated for these different sulfide phases using the CrystalMaker software program SingleCrystal.

Results & Discussion: Two FIB sections from the particle C0076-FO004 are dominated by a groundmass of phyllosilicates with abundant sulfides and minor magnetite and carbonate. Olivine and pyroxene are absent. There are two different occurrences of phyllosilicates (**Fig. 1a**): (1) irregularly-shaped, denser aggregates of coarsely-crystallized phyllosilicates that are free of sulfide grains and (2) poorly-crystallized, fine-grained phyllosilicates associated with numerous nanometer-sized sulfide grains. Basal spacings of 7 Å and 10 Å are commonly observed in both occurrences, indicating coherent, disordered intergrowths of serpentine and saponite as the main hydrous phases. These observations are similar to general features observed from Orgueil matrix [5], except that ferrihydrite of probable terrestrial weathering origin is absent in our FIB sections. As proposed by [5], the Ryugu particle studied may have experienced pervasive but incomplete aqueous alteration that resulted in a partial replacement of coarsely-crystallized phyllosilicates by fine-grained assemblages of poorly-crystallized phyllosilicates and sulfide grains. Alternatively, coarsely-crystallized phyllosilicates may have formed as alteration became more advanced.

Sulfide grains in the particle C0076-FO004 are generally euhedral, having tabular to polygonal morphologies, typical of CI sulfides [6]. Among 12 crystals analyzed so far, we identified ten as pyrrhotite and two as pentlandite. Likewise, pyrrhotite occurs as the most common sulfide phase in CIs and pentlandite as a minor phase [6].

TEM EDX analysis of pyrrhotite grains in the particle C0076-FO004 shows that their Ni contents are typically low (0.8-1 wt%), consistent with those of CI pyrrhotites [6-8], but can increase up to 6 wt%. There is no evidence for the presence of pentlandite inclusions or exsolution lamellae in these pyrrhotite grains, which are common in CM pyrrhotites [9]. Such Ni-rich pyrrhotite

with up to 16 at% Ni was reported from Orgueil [7]. In addition, pyrrhotite grains in the particle C0076-FO004 have variable metal-to-sulfur ratios of 0.87 to 1. Their Fe/S ratios range from 0.85 to 1, with most being near ~0.9. This observed range is similar to that (Fe/S = 0.8 to <0.98) of pyrrhotite measured by EPMA from CIs and CMs [8]. However, the observed compositional variation in pyrrhotites from the Ryugu particle suggests a local heterogeneity in aqueous alteration conditions.

Thorough analysis of SAED and FFT patterns obtained from ten pyrrhotite grains in the particle C0076-FO004 revealed that all crystals have the monoclinic 4C structure (Figs. 1b-c). Three pyrrhotite crystals are twinned, as indicated by the intergrown [110] and [010] zone axes in diffraction patterns (Fig. 1b). They show streaking along c^* in diffraction patterns and linear features along the (001) plane in scanning TEM imaging, due to twinning or disorder in the distribution of Fe-site vacancies [9]. In addition, high-resolution TEM imaging displays consistent d-spacings throughout individual pyrrhotite crystals, together with their sharp and consistent diffraction spots, indicating that they are single crystals of a well-ordered, uniform structure. These observations suggest that pyrrhotite formed below ~250°C [10], and was never subsequently heated enough for any structural change from 4C to metal-rich 5C or 6C. As observed in CIs [7], Ni had preferentially substituted for Fe^{3+} and filled ordered vacancies, resulting in an increase in Ni contents and metal-to-sulfur ratios.

In addition, two pentlandite grains are identified in our FIB sections as isolated grains in the matrix, and diffraction patterns obtained from one crystal match well with its isometric structure (Fig. 1d). They contain 10 wt% and 22 wt% Ni, respectively, lower values than

expected for stoichiometric pentlandite of ~32 wt%. However, metal-to-sulfur ratios of the pentlandite grains are 1.05 and 1.1, respectively, which are similar to values from Orgueil pentlandites [7]. Such Ni deficiencies were also reported in Alais pentlandites (22-27 wt% Ni) [6].

In the particle C0076-FO004, two carbonate grains (~1-3 μm in size) are observed as isolated dolomite phase in the matrix. They have slightly different compositions of $(\text{Ca}_{0.51}\text{Mg}_{0.41}\text{Mn}_{0.04}\text{Fe}_{0.04})\text{CO}_3$ and $(\text{Ca}_{0.48}\text{Mg}_{0.44}\text{Mn}_{0.04}\text{Fe}_{0.03})\text{CO}_3$, which are within the range reported from CI dolomites [11]. One magnetite spray is present and is essentially pure Fe_3O_4 . Carbonaceous material occurs as nanoglobules: three have a hollow shape, while one appears an aggregate of a few globules.

Conclusions: The Ryugu particle C0076-FO004 analyzed for this FIB/TEM study provides mineralogical and chemical evidence that this particle is CI-like material that experienced extensive but heterogeneous aqueous alteration below ~250°C [4]. Further analysis is underway to better characterize the structures and non-stoichiometric compositions of pyrrhotite and pentlandite grains.

References: [1] Arakawa M. et al. (2020) *Science* 368, 67-71. [2] Pilorget C. (2021) *Nat Astron.* [3] Yada T. et al. (2021) *Nat Astron.* [4] Nakamura T. et al. (2022) *Science*, submitted. [5] Tomeoka K. and Buseck P. R. (1988) *GCA* 52, 1627-1640. [6] Bullock E. A. et al. (2005) *GCA* 69, 2687-2700. [7] Berger E. L. et al. (2016) *MAPS* 51, 1813-1829. [8] Schrader D. L. et al. (2021) *GCA* 303, 66-91. [9] Harries D. and Zolensky M. E. (2016) *MAPS* 51, 1096-1109. [10] Kissin S. A. and Scott S. D. (1982) *Econ Geol* 77, 1739-1754. [11] Brearley A. J. and Jones R. H. (1998) *In Planetary Materials*. pp. 3-191-3-244.

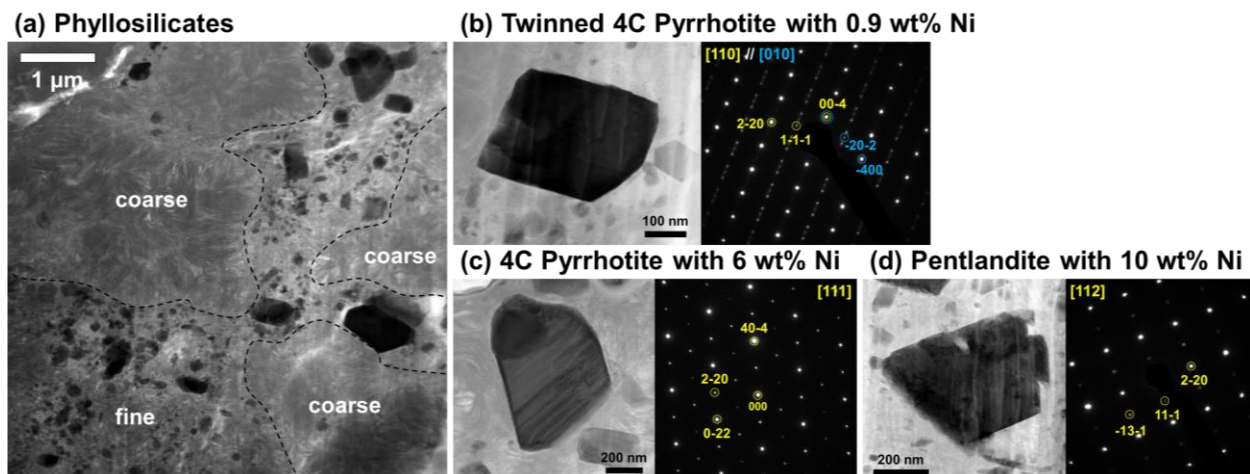


Figure 1. (a) Bright-field scanning TEM image of coarse and fine phyllosilicates. Abundant sulfide grains are distributed only in the regions of fine phyllosilicates. (b-d) Bright-field scanning TEM images of pyrrhotite and pentlandite grains and their diffraction patterns. All pyrrhotite crystals analyzed have the monoclinic 4C structure.